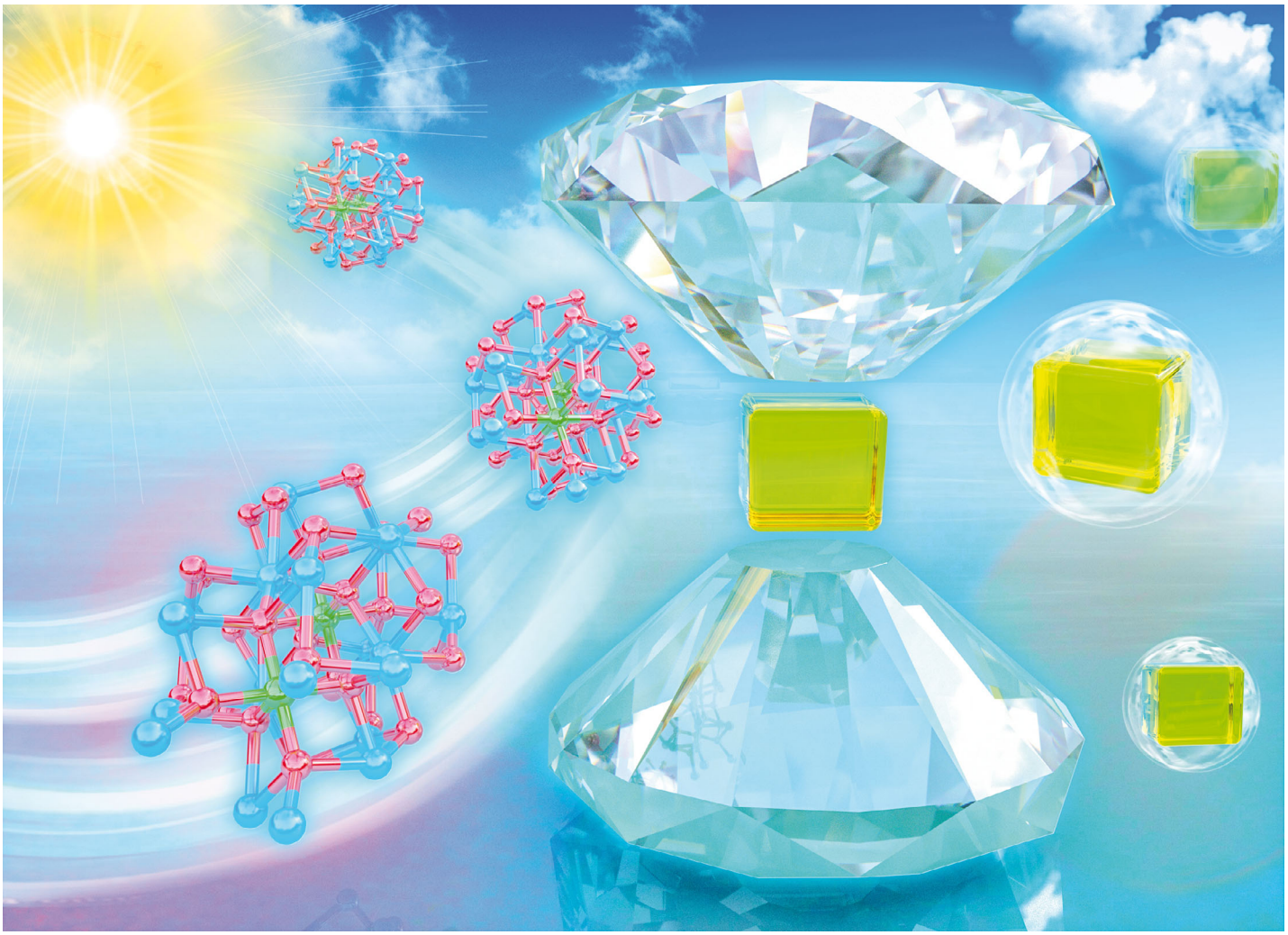

Showcasing research from Professor Peter Lazor's laboratory, Department of Earth Sciences, Uppsala University, Uppsala, Sweden.

Bandgap engineering in Mn_3TeO_6: giant irreversible bandgap reduction triggered by pressure

A pressure-induced structural change in the multiferroic oxide Mn_3TeO_6 yields formation of a novel compound whose broad optical absorption band matches closely to the solar radiation spectrum. Importantly, the compound's stability after a complete pressure release renders it a promising light-harvesting material for solar cells.

As featured in:

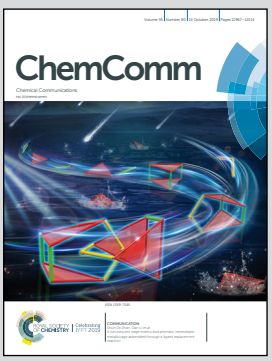

See Lei Liu, Peter Lazor *et al.*, *Chem. Commun.*, 2019, **55**, 12000.

ROYAL SOCIETY OF CHEMISTRY | Celebrating IYPT 2019

rsc.li/chemcomm

Registered charity number: 207890

ChemComm

COMMUNICATION

View Article Online
View Journal | View Issue

Cite this: *Chem. Commun.*, 2019, **55**, 12000

Received 23rd June 2019,
Accepted 3rd September 2019

DOI: 10.1039/c9cc04821a

rsc.li/chemcomm

Bandgap engineering in Mn_3TeO_6: giant irreversible bandgap reduction triggered by pressure†

Lei Liu, *[a] Henrik Skogby,[b] Sergey Ivanov,[cd] Matthias Weil,[e] Roland Mathieu[c] and Peter Lazor*[a]

In this study, the bandgap energy of the multiferroic oxide Mn_3TeO_6 is successfully reduced by ~39% from 3.15 eV to 1.86 eV, accompanied by a phase transition at high pressures. The high-pressure phase with smaller bandgap energy is quenchable to ambient conditions and represents a promising light-harvesting material for photovoltaic applications.

For semiconductors, the bandgap is arguably the most decisive parameter for their applications, including the photovoltaic effect in solar cells,[1] where light-harvesting materials represent the key parts. In the past decade, organic–inorganic halide perovskites have emerged as extraordinary candidates for solar absorbers. Today, their power conversion efficiency (PCE) approaches 23.7%, becoming comparable to the performance of crystalline Si cells.[2] However, several drawbacks of this category of perovskites (*e.g.*, degradation, hysteresis, and lead pollutions) hinder their further commercialization.[3–6] Consequently, major efforts are devoted to searching for environmentally friendly and stable light-harvesting materials.

Recent investigations demonstrated that multiferroic oxides might represent a potential alternative for the organic–inorganic halide perovskites used in solar cell applications.[7,8] The PCE of the Bi_2CrFeO_6-based perovskite solar cell has reached a value as high as 8.1%. Unfortunately, wide bandgaps (2.7–4.0 eV) of multiferroic oxides prevent the further improvement of the photovoltaic efficiency. According to previous studies, four methods may aid in reducing the bandgaps of perovskite oxides or other oxides with similar building blocks:[9] (1) increasing the dimensionality of the BO_6 network;[10] (2) increasing the B–O–B bonding angle;[11] (3) decreasing the electronegativity of anions,[12–16] and (4) decreasing the effective electronegativity discrepancy between the metal (B) cation and the anion. Parameters in the first two methods correlate closely with the underlying crystal structure, which can be significantly influenced by means of pressure.[17,18] Consequently, pressure assisted engineering of multiferroic perovskite oxides or related materials offer a promising approach to synthesize light-harvesting materials with appropriate bandgaps for photovoltaic applications. However, this topic has not yet been addressed to date.

In the present study, pressure was used to tune the crystal structure, and concomitantly the bandgap of the multiferroic oxide $Mn_3^{II}Te^{VI}O_6$ (MTO). MTO crystallizes in the $R\bar{3}$ space group type under ambient conditions with TeO_6 octahedra and considerably distorted MnO_6 octahedra.[19–22] Raman spectra collected from the sample under successively increased compressions show a phase transition at ~16–18 GPa. Results of UV-vis absorption spectroscopy reveal a bandgap reduction of 0.98 eV from 3.15 eV to 2.17 eV, accompanying the phase transition. Significantly, the high-pressure phase showed up to be quenchable to ambient conditions with the bandgap further decreasing to 1.86 eV. These findings demonstrate that pressure can represent a clean and efficient tool for tuning the bandgaps of materials, and that quenched MTO may be a promising light-harvesting material and environmentally benign optoelectronic material in the future.

Fig. 1(a and b) show the *in situ* Raman spectra of MTO during compression to 40.54 GPa and decompression to 0.33 GPa in a diamond anvil cell. In the pressure range of ~16–18 GPa, a group of Raman modes spanning ~178–323 cm^{-1} becomes silent and remains absent upon further pressure increase. Additionally, the two strongest Raman bands at ~780–820 cm^{-1} disappear, and a new much broader strong band gradually emerges at lower wavenumbers of ~765–778 cm^{-1}. These two features indicate a phase transition in the aforementioned pressure range. The Raman band positions of MTO as a function of pressure upon compression are plotted in Fig. 1(c) along with the highlighted

[a] *Department of Earth Sciences, Uppsala University, Uppsala 75236, Sweden. E-mail: lei.liu@geo.uu.se, peter.lazor@geo.uu.se*
[b] *Department of Geosciences, Swedish Museum of Natural History, Stockholm, 10405, Sweden*
[c] *Department of Engineering Sciences, Uppsala University, Box 534, Uppsala 75121, Sweden*
[d] *Department of Inorganic Materials, Karpov's Institute of Physical Chemistry, Vorontsovo pole, Moscow 105046, Russia*
[e] *Institute for Chemical Technologies and Analytics, TU Wien, Getreidemarkt 9/164-SC, Vienna A-1060, Austria*

† Electronic supplementary information (ESI) available: Detailed synthesis and *in situ* high-pressure Raman and UV-vis absorption experiment methods. See DOI: 10.1039/c9cc04821a

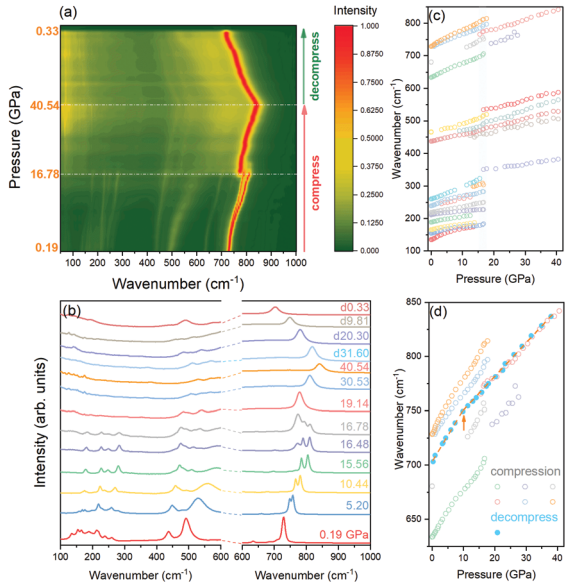

Fig. 1 (a) Contour plot of 2D normalized Raman spectra of MTO during compression to 40.54 GPa, and then decompressed to 0.33 GPa, (b) 1D Raman spectra of MTO during compression and decompression (two different intensity scales apply below and above 600 cm^{-1}), and (c) Raman peak positions as a function of pressure. The shaded area highlights the phase transition region. (d) Portions of selected strong Raman bands as a function of pressure upon compression (open circles), and decompression (solid circles). The arrow marks a change in the slope.

phase transition region. A sizeable decrease of the observed Raman modes in the high-pressure phase may originate from its higher symmetry as compared to the parent phase. Upon decompression, the strongest broad band survives, and the group of low energy modes keeps silent to the pressure as low as 0.33 GPa. Hence, the high-pressure phase is quenchable to almost ambient pressure, indicating irreversibility of the transition. Fig. 1(d) shows that the position of the strongest Raman band of the high-pressure phase upon decompression retraces those upon compression. A subtle change in the slope occurs in the pressure range of 7.32–9.81 GPa, as marked by the arrow. In MTO, the strongest bonding is within the Te–O link.[22] The intense Raman band with the highest wavenumber is assigned to the Te–O symmetric stretching of the TeO_6 octahedra.[23–25] Possibly, the detected slope change arises from a slight alteration of the shape of TeO_6 and/or MnO_6 octahedra in MTO. A further examination of the crystal structure, ideally using X-ray diffraction on a single crystal is required in order to explain the nature of the high-pressure phase and the origin of this feature.

In situ optical observations of the sample compressed in the diamond anvil cell revealed a pressure-induced piezochromic effect accompanying the phase transition (Fig. 2). At low pressure, the MTO single crystal displays an almost colourless appearance when viewed in transmission mode using white light. Upon compression, in the phase transition region of ~16–18 GPa, the crystal colour becomes light brown and turns darker and darker as pressure increases. This observation can be explained by the progressively higher absorption of light due to the narrowing bandgap of the high-pressure phase. Upon decompression,

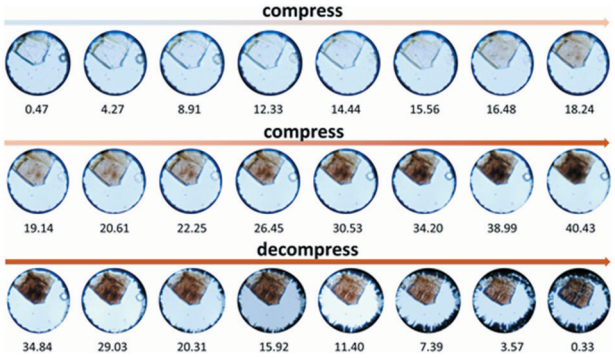

Fig. 2 Optical transmitted-light micrographs of a MTO single crystal view through a diamond anvil cell in the course of compression and decompression in a silicone oil pressure medium. The diameter of the sample chamber is around 110 μm.

the dark brown colour of the crystal does not exhibit an obvious reverse change, even to a pressure as low as 0.33 GPa. This feature of the piezochromic effect lends further support for the irreversibility of the observed pressure-induced phase transition.

Aiming at the quantitative characterization of the bandgap variation of MTO under compression and decompression, we carried out a UV-vis absorption experiment. The UV-vis spectra of MTO collected under compression to 34.45 GPa, followed by measurements upon pressure release up to the ambient pressure are shown in Fig. 3(a). Only one absorption band at ~343 nm is found up to 18.03 GPa. Its position remains constant as pressure increases. As shown in Fig. 3(c), the location

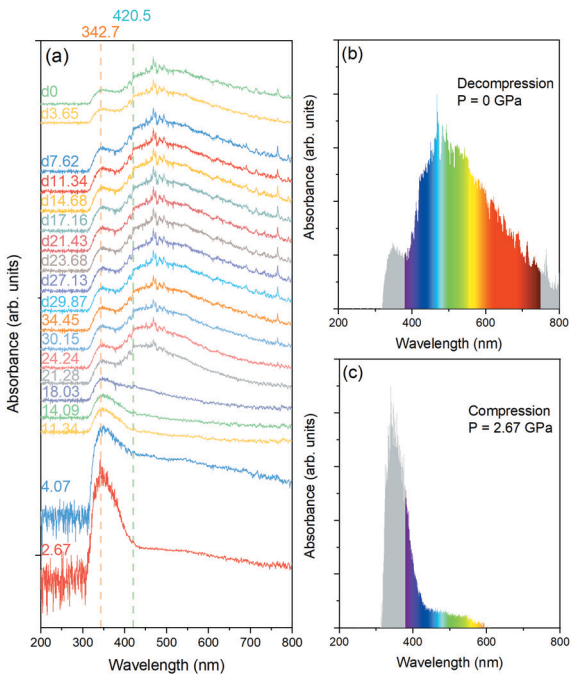

Fig. 3 (a) UV-vis absorption spectra of MTO taken during compression to 34.45 GPa and decompression to ambient pressure, (b) UV-vis spectra of MTO released to ambient pressure, and (c) UV-vis spectra of MTO at 2.67 GPa, collected upon pressure increase.

of the band in the UV region implies absorption of only a small portion of the visible light by the crystal, rendering it unsuitable for photovoltaic applications. According to the aforementioned Raman spectroscopy results, at pressures higher than 18.03 GPa, MTO adopts another phase. At 21.28 GPa, a new absorption band appears at ~420 nm, arising possibly from the distortion of the MnO_6 and/or TeO_6 polyhedra, or charge transfer between the ions.[26] The absorption spectra seem almost unchanged upon compression up to the highest pressure of 34.45 GPa, and even after the complete pressure release. The absorption spectrum of the quenched MTO is shown in Fig. 3(b). The main absorption band has a maximum at ~480 nm, and covers the entire visible light range, indicating that the quenched MTO is a promising light-harvesting material for solar cells.

The Tauc plots are employed to determine the bandgap energy of MTO using the direct allowed transition models in Fig. 4(a).[27] The absorption edges abruptly jump to lower energy after the phase transition. The bandgap energy as a function of pressure is shown in Fig. 4(b). The bandgap energy of the low-pressure phase is higher than 3 eV. During the phase transition, the energy decreases, ΔE_g = 0.98 eV, from 3.15 eV at 18.03 GPa to 2.17 eV at 21.28 GPa. The bandgap energy of the high-pressure phase decreases as pressure increases and reaches 2.07 eV at the highest experimental pressure of 34.45 GPa.

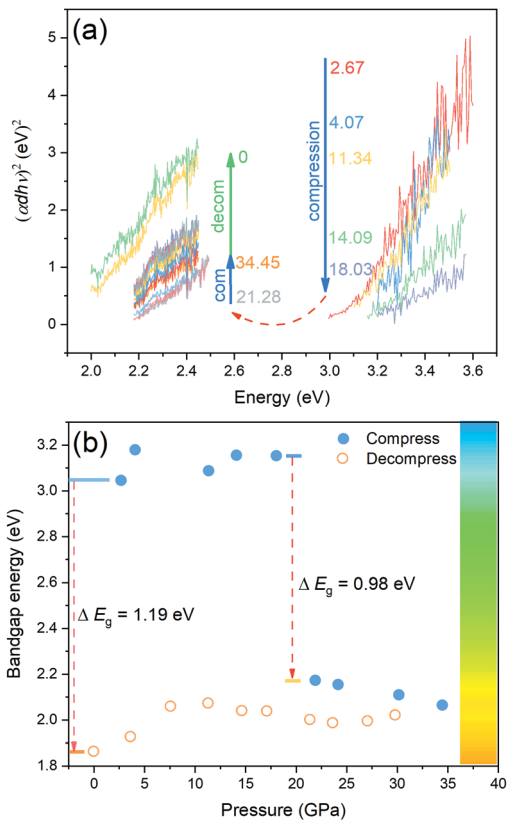

Fig. 4 (a) The linear part in the Tauc plot used for fitting the bandgap energy of MTO during compression and decompression. The plot at 2.67 GPa is multiplied by 0.1 for clarity. (b) The bandgap energy of MTO during compression and decompression.

Upon decompression, the bandgap energy remains almost unchanged to 11.34 GPa (E_g = 2.07 eV). At lower pressures, the energy decreases upon pressure decrease and reaches 1.86 eV at ambient pressure. The bandgap–pressure relationship shows a kink in the pressure range of 7.62–11.34 GPa, which agrees well with the Raman position–pressure relationship kink shown in Fig. 1(d) in the pressure range of 7.32–9.81 GPa.

In this work, we used pressure to tailor the bandgap energy of the multiferroic oxide MTO. Nearly 1 eV optical bandgap reduction has been discovered due to the pressure-induced phase transition at ~16–18 GPa, as evidenced by UV-vis absorption measurements and Raman spectroscopy results. The quenched MTO exhibiting bandgap energy of 1.86 eV represents a promising light-harvesting material for photovoltaic applications. This result opens a green way for tuning the bandgap energies of multiferroic oxides, which are considered as stable and nontoxic alternatives of the organic–inorganic halide perovskites.

This work was supported by Uppsala University and the Swedish Research Council (VR). The authors would like to thank Professor Ulf Hålenius for the useful discussion on the absorption spectrum of MTO.

Conflicts of interest

There are no conflicts to declare.

Notes and references

1 C. Ning, L. Dou and P. Yang, *Nat. Rev. Mater.*, 2017, **2**, 17070.
2 National Renewable Energy Laboratory, Best research-cell efficiency chart, 2019, https://www.nrel.gov/pv/assets/pdfs/pv-efficiency-chart.20181221.pdf.
3 M. Grätzel, *Nat. Mater.*, 2014, **13**, 838.
4 T. Zhang, H. Chen, Y. Bai, S. Xiao, L. Zhu, C. Hu, Q. Xue and S. Yang, *Nano Energy*, 2016, **26**, 620.
5 H. Chen, X. Zheng, Q. Li, Y. Yang, S. Xiao, C. Hu, Y. Bai, T. Zhang, K. S. Wong and S. Yang, *J. Mater. Chem. A*, 2016, **4**, 12897.
6 L. Meng, J. You and Y. Yang, *Nat. Commun.*, 2018, **9**, 5265.
7 I. Grinberg, D. V. West, M. Torres, G. Gou, D. M. Stein, L. Wu, G. Chen, E. M. Gallo, A. R. Akbashev, P. K. Davies, J. E. Spanier and A. M. Rappe, *Nature*, 2013, **503**, 509.
8 R. Nechache, C. Harnagea, S. Li, L. Cardenas, W. Huang, J. Chakrabartty and F. Rosei, *Nat. Photonics*, 2015, **9**, 61.
9 P. Gao, M. Grätzel and M. K. Nazeeruddin, *Energy Environ. Sci.*, 2014, **7**, 2448.
10 Y. Takeoka, K. Asai, M. Rikukawa and K. Sanui, *Bull. Chem. Soc. Jpn.*, 2006, **79**, 1607.
11 J. L. Knutson, J. D. Martin and D. B. Mitzi, *Inorg. Chem.*, 2005, **44**, 4699.
12 H. W. Eng, P. W. Barnes, B. M. Auer and P. M. Woodward, *J. Solid State Chem.*, 2003, **175**, 94.
13 J. Etourneau, J. Portier and F. Menil, *J. Alloys Compd.*, 1992, **188**, 1.
14 M. Jansen and H. P. Letschert, *Nature*, 2000, **404**, 980.
15 E. Knittle and R. Jeanloz, *Science*, 1987, **235**, 668.
16 R. Marchand, F. Tessier, A. Le Sauze and N. Diot, *Int. J. Inorg. Mater.*, 2001, **3**, 1143.
17 G. Shen and H. K. Mao, *Rep. Prog. Phys.*, 2017, **80**, 016101.
18 H. K. Mao, X. Chen, Y. Ding, B. Li and L. Wang, *Rev. Mod. Phys.*, 2018, **90**, 015007.
19 L. Zhao, Z. Hu, C. Kuo, T. Pi, M. Wu, L. Tjeng and A. C. Komarek, *Phys. Status Solidi RRL*, 2015, **9**, 730.
20 S. A. Ivanov, C. Ritter, P. Nordblad, R. Tellgren, M. Weil, V. Carolus, T. Lottermoser, M. Fiebig and R. Mathieu, *J. Phys. D: Appl. Phys.*, 2017, **50**, 085001.

21 S. A. Ivanov, P. Nordblad, R. Mathieu, R. Tellgren, C. Ritter, N. V. Golubko, E. D. Politova and M. Weil, *Mater. Res. Bull.*, 2011, **46**, 1870.
22 M. Weil, *Acta Crystallogr., Sect. E: Struct. Rep. Online*, 2006, **62**, i244.
23 M. Liegeois-Duyckaerts and P. Tarte, *Spectrochim. Acta, Part A*, 1974, **30**, 1771.
24 A. P. Ayala, I. Guedes, E. N. Silva, M. S. Augsburger, M. del, C. Viola and J. C. Pedregosa, *J. Appl. Phys.*, 2007, **101**, 123511.
25 R. L. Andrews, A. M. Heyns and P. M. Woodward, *Dalton Trans.*, 2015, **44**, 10700.
26 P. Jiang, J. Li, A. W. Sleight and M. A. Subramanian, *Inorg. Chem.*, 2011, **50**, 5858.
27 J. Tauc, *Mater. Res. Bull.*, 1968, **3**, 37.